Identification of space- and temperature-dependent heat transfer coefficient

Farzad Mohebbi*, Mathieu Sellier

Department of Mechanical Engineering, University of Canterbury, Private Bag 4800, Christchurch 8140, New Zealand

Abstract. The aim of this paper is to present a very efficient and accurate numerical algorithm to identify a variable (space- and temperature-dependent) heat transfer coefficient in two-dimensional inverse steady-state heat conduction problems involving irregular heat-conducting body shapes in the presence of Dirichlet, Neumann, and Robin boundary conditions. In this numerical method, a boundary-fitted grid generation technique (elliptic) is used to discretize the physical domain (heat-conducting body) and solve for the steady-state heat conduction equation by approximating the derivatives of the field variable (temperature) by algebraic ones. This paper describes a very accurate and efficient sensitivity analysis scheme to compute the sensitivity of the temperatures to variation of the variable heat transfer coefficient. The main advantage of the sensitivity analysis scheme is that it does not require the solution of adjoint equation. The conjugate gradient method (CGM) is used to reduce the mismatch between the computed temperature on part of the boundary and the simulated measured temperature distribution. The obtained results confirm that the proposed algorithm is very accurate, efficient, and robust.

Keywords. Inverse Heat Transfer, Elliptic Grid Generation, Sensitivity Analysis, Variable Heat Transfer Coefficient, Conjugate Gradient Method

---

*Corresponding author.

E-mail address: farzadmohebbi@yahoo.com

NOMENCLATURE:

$d^{(\mathrm{k})}$	direction of descent at iteration k
$\dot{q}$	heat flux $(\frac{\mathrm{W}}{\mathrm{m}^2})$
h	heat transfer coefficient $(\frac{\mathrm{W}}{\mathrm{m}^2.^\circ\mathrm{C}})$
Ja	Jacobian matrix
J	Jacobian of transformation
$\mathcal{J}$	objective function
k_T	thermal conductivity of the solid body $(\frac{\mathrm{W}}{\mathrm{m}.^\circ\mathrm{C}})$
n	outward drawn unit vector
T	temperature ($^\circ$C)
T_m	measured outer surface temperature ($^\circ$C)
T_∞	ambient temperature ($^\circ$C)
x, y	Cartesian coordinates in the physical domain

Greek symbols

α, β, γ	metric coefficients in 2-D elliptic grid generation
$\beta^{(\mathrm{k})}$	search step size at iteration k
Γ	boundary
$\gamma^{(\mathrm{k})}$	conjugation coefficient at iteration k
Ω	domain
ξ, η	Cartesian coordinates in the computational domain

Subscripts

i	grid index in ξ- direction
j	grid index in η- direction
M	number of grid points in the ξ- direction
N	number of grid points in the η- direction

Superscript

k	iteration number

1. Introduction

Inverse Heat Transfer Problems (IHTPs) are widely considered mathematically challenging problems. IHTPs are ill-posed and difficult to solve. Ill-posed problems are inherently unstable and very sensitive to noise. In other words, in such problems a small error in the input data can give rise to a large error in the solution [1-3]. Therefore, the development of efficient, accurate, and robust numerical schemes to solve IHTPs is of vital importance. Direct well-posed heat transfer problems are concerned with the determination of the temperature distribution over a heat-conducting body given that the boundary conditions, the thermo-physical properties, the geometrical configuration of the body, and the applied heat flux are all known. In contrast, the inverse heat transfer problem deals with the determination of the boundary conditions, the thermo-physical properties, the geometrical configuration of the heat-conducting body, and the applied heat flux from the knowledge of the temperature distribution on some part of the body boundary. Inverse heat transfer analysis has been extensively used to determine the thermo-physical properties such as the thermal conductivity and the convection heat transfer coefficient [4-29], the heat flux [18, 29-36], and the boundary shape of bodies [37-43]. The evaluation of the convection heat transfer coefficient is a difficult task because convection is a very complex phenomenon [44]. The convection heat transfer coefficient depends on many variables such as the geometry of the surface as well as the surface temperature, to name a few. The estimation of a variable convection heat transfer coefficient using an inverse analysis has been less researched [45-48]. In the literature, there exist some limitations on the proposed methods by different researchers to identify such a variable parameter. Some of these limitations can be summarized as follows:

- the applicability of the direct solver to rectangular or circular heated bodies only (using traditional finite-difference method) and inability to consider a general 2D domain.

- the inability to handle a variety of boundary conditions. Most of the boundary conditions in the literature include a constant temperature (Dirichlet boundary condition) or insulated case.

Thus a general methodology for a *general* 2D domain and boundary conditions considering a variable convection heat transfer coefficient with a high degree of accuracy is required. This paper deals with a two dimensional inverse steady-state heat conduction problem. The objective of this study is to estimate a variable (space- and temperature-dependent) heat transfer coefficient in an irregular body. The convection heat transfer coefficient considered in this paper is a linearly space (boundary surface shape)- and temperature (boundary surface temperature)-dependent parameter. However, the linear from can be easily extended to other forms of dependency of the convective heat transfer coefficient on the space and temperature such as quadratic and cubic.

In the proposed numerical approach, an elliptic grid generation technique is used to generate a mesh over the irregular body and solve for the steady state heat conduction equation. The discretization in the computational domain is based on the finite-difference method, a method chosen for its simplicity and ease of implementation. The most innovative aspect of the numerical approach is its very efficient and accurate sensitivity analysis scheme, already introduced by the authors for other parameter estimation problems in heat transfer [18, 28, 29]. The sensitivity analysis scheme is formulated to compute the sensitivity of the temperatures to variation of the variable heat transfer coefficient. The conjugate gradient method is employed to minimize the difference between the computed temperature on part of the boundary and the simulated measured temperature. As will be shown, this numerical methodology does not require the solution of an adjoint problem. Explicit expressions for the sensitivity coefficients are derived which allow for the computation of the sensitivity coefficients in one single solve.

The proposed solution method introduced here is sufficiently general and can be employed for the estimation of a space- and temperature-dependent heat transfer coefficient applied on part of the boundary of a *general* two-dimensional region as long as the general two-dimensional region can be mapped onto a regular computational domain. Moreover, there is no limitation on the type of the boundary conditions. In other words, Dirichlet, Neumann, and Robin boundary conditions can be imposed on the domain boundary.

2. Governing equation

The mathematical representation of the steady-state heat conduction problem of interest here can be expressed as below (see Fig. 1)

$$\nabla^2 T = 0 \text{ in physical domain } \Omega \tag{1}$$

subject to the boundary conditions

$$\frac{\partial T}{\partial n} = -\frac{\dot{q}}{k_T} \text{ on boundary surface } \Gamma_1 \tag{2}$$

$$\frac{\partial T}{\partial n} = -\frac{h_i}{k_T}(T_{\Gamma_i} - T_{\infty_i}) \text{ on boundary surface } \Gamma_i,\ i = 3,4 \tag{3}$$

Two different cases are considered for the boundary condition on the boundary surface Γ_2 which will be considered separately:

Case 1: The heat transfer coefficient is space-dependent (Fig. 1a):

$$\frac{\partial T}{\partial n} = -\frac{h_2(\Gamma_2)}{k_T}\left(T_{\Gamma_2} - T_{\infty_2}\right) \text{ on boundary surface } \Gamma_2 \tag{4}$$

where $h_2(\Gamma_2) = a_1 X_{\Gamma_2} + a_2 Y_{\Gamma_2} + a_3$.

Case 2: The heat transfer coefficient is temperature-dependent (Fig. 1b):

$$\frac{\partial T}{\partial n} = -\frac{h_2(T_{\Gamma_2})}{k_T}\left(T_{\Gamma_2} - T_{\infty_2}\right) \text{ on boundary surface } \Gamma_2 \tag{5}$$

where $h_2(T_{\Gamma_2}) = a + bT_{\Gamma_2}$.

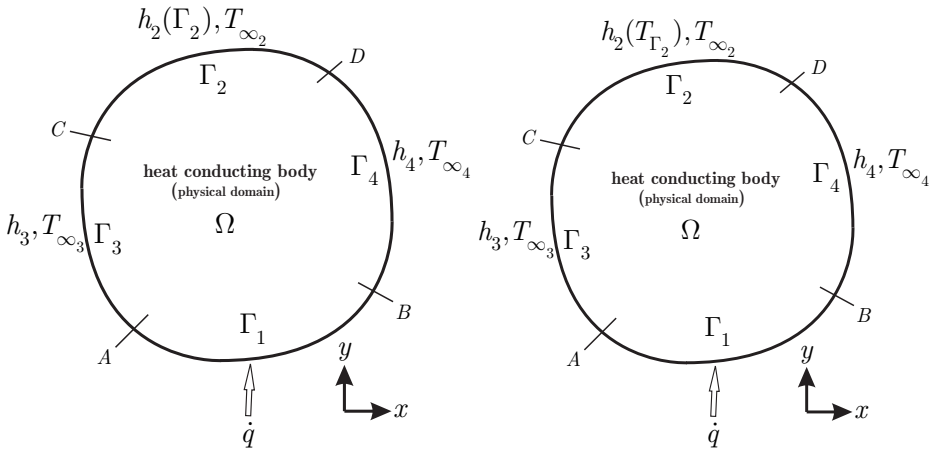

Fig. 1 Physical domain (solid body) subjected to convective heat transfer on surfaces Γ_i, $i = 2,3,4$ and heat flux $\dot{q}$ on surface Γ_1. The thermal conductivity of the body is k_T .

In this study, the elliptic grid generation technique is employed to discretize the physical domain and approximate the derivatives of the field variable (temperature) by algebraic ones. This technique is based on solving a system of elliptic partial differential equations to distribute nodes in the interior of the physical domain by mapping the irregular physical domain from the x and y physical plane (Fig. 1) onto the ξ and η computational plane (Fig. 2), which is a regular region [49].

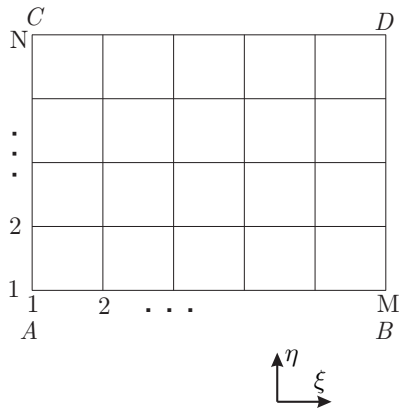

Fig. 2 Computational domain.

More details on the implementation of the elliptic grid generation technique and solution procedure for the steady-state heat conduction equation can be found in [50].

3. The inverse analysis

3.1. Objective function

An inverse analysis can be used to estimate the variable heat transfer coefficient h_2 (using the estimation of a_1, a_2, a_3 for the space-dependent heat transfer coefficient and a and b for the temperature-dependent heat transfer coefficient separately) so that the square of the difference between the computed temperature of the outer surface Γ_2 and the measured temperature of the same surface is minimized. This can be mathematically expressed as

$$\min \left\{ \underset{h_2 \text{ on } \Gamma_2}{\mathcal{J}} := C \left\| T_{\Gamma_2} - T_m \right\|^2 : \text{Eq.(1) in } \Omega, \text{ BCs in Eqs.(2)-(4) or (5)} \right\} \qquad (6)$$

where C is a positive constant and can be considered as $C = 10^n, n = 0,1,2,\ldots$. The aim of the inverse analysis is to minimize the following objective function expression using the optimization of the value of a_1, a_2, a_3 for the space-dependent h_2 and a and b for the temperature-dependent h_2:

$$\mathcal{J} = C\sum_{i=2}^{M-1}(T_{i,N} - T_{(i,N)_m})^2 \tag{7}$$

3.2 Sensitivity analysis

As the proposed method is concerned with a gradient-based optimization method (here, conjugate gradient method), the computation of derivative of the objective function with respect to the unknown variables is needed. Since two different cases are considered for the variable heat transfer coefficient, two different sensitivity analysis schemes are considered as follows:

Case 1) Space-dependent heat transfer coefficient $h_2(\Gamma_2) = a_1 X_{\Gamma_2} + a_2 Y_{\Gamma_2} + a_3$:

In this case, the sensitivity of the objective function $\mathcal{J}$ defined by Eq.(7) to the unknown variables a_1, a_2, a_3 is calculated as follows

$$\frac{\partial \mathcal{J}}{\partial a_l} = 2C\sum_{i=2}^{M-1}(T_{i,N} - T_{(i,N)_m})\frac{\partial T_{i,N}}{\partial a_l} = 2\sum_{i=2}^{M-1}(T_{i,N} - T_{(i,N)_m})C\frac{\partial T_{i,N}}{\partial a_l} \tag{8}$$

where $l = 1,2,3$. In Eq. (8), $C\dfrac{\partial T_{i,N}}{\partial a_l}$ $(l = 1,2,3)$ are called the sensitivity coefficients. To obtain an algebraic expression for the sensitivity coefficients, from the boundary condition of the heat conduction equation at the surface Γ_2, Eq. (4), we have

$$\dot{q}_{\text{conduction}}\,|_{\Gamma_2} = \dot{q}_{\text{convection}}\,|_{\Gamma_2}$$

$$-k_T\frac{\partial T}{\partial n_2} = h_2(T_{\Gamma_2} - T_{\infty_2})$$

$$-k_T\frac{\partial T}{\partial n_2} = (a_1 X_{\Gamma_2} + a_2 Y_{\Gamma_2} + a_3)(T_{\Gamma_2} - T_{\infty_2}) \tag{9}$$

The term $\frac{\partial T}{\partial n}$ at a boundary surface in the physical domain is related to $\frac{\partial T}{\partial \xi}$ and/or $\frac{\partial T}{\partial \eta}$ at the corresponding transformed boundary surface in the computational domain. At surface Γ_2 we have

$$\frac{\partial T}{\partial n}\Big|_{\Gamma_2} = \frac{\partial T}{\partial \eta}\Big|_{\Gamma_2} = \frac{1}{J\sqrt{\gamma}}(\gamma T_\eta - \beta T_\xi) \tag{10}$$

where (from the elliptic grid generation method)

$$\alpha = x_\eta^{\,2} + y_\eta^{\,2}, \beta = x_\xi x_\eta + y_\xi y_\eta, \gamma = x_\xi^{\,2} + y_\xi^{\,2}, J = x_\xi y_\eta - x_\eta y_\xi \tag{11}$$

Using the finite-difference method, the T_η and T_ξ at every boundary surface with Neumann and Robin conditions can be discretized. By substituting Eq. (10) and the finite-difference expressions for T_ξ and T_η (on the boundary surface Γ_2) into Eq. (9), we get

$$-k_T\left[\frac{1}{J\sqrt{\gamma}}\left(\gamma\frac{3T_{i,N} - 4T_{i,N-1} + T_{i,N-2}}{2} - \beta\frac{T_{i+1,N} - T_{i-1,N}}{2}\right)\right] = (a_1 x_{i,N} + a_2 y_{i,N} + a_3)\left(T_{i,N} - T_{\infty_2}\right) \tag{12}$$

The following expression is obtained by solving Eq. (12) in terms of $T_{i,N}$:

$$T_{i,N} = \frac{(4k_T\gamma T_{i,N-1} - k_T\gamma T_{i,N-2} + k_T\beta T_{i+1,N} - k_T\beta T_{i-1,N} + 2J\sqrt{\gamma}a_1 x_{i,N}T_{\infty_2} + 2J\sqrt{\gamma}a_2 y_{i,N}T_{\infty_2} + 2J\sqrt{\gamma}a_3 T_{\infty_2})}{(3k_T\gamma + 2J\sqrt{\gamma}a_1 x_{i,N} + 2J\sqrt{\gamma}a_2 y_{i,N} + 2J\sqrt{\gamma}a_3)} \tag{13}$$

Using an algebraic software, one can obtain an expression for the sensitivity coefficients $C\dfrac{\partial T_{i,N}}{\partial a_l}$ $(l=1,2,3)$ by differentiating the obtained expression for $T_{i,N}$ with respect to a_1, a_2, and a_3, respectively, as follows

$$\frac{\partial T_{i,N}}{\partial a_1}=\frac{2J\sqrt{\gamma}x_{i,N}k_T(3T_{\infty_2}\gamma-4\gamma T_{i,N-1}+\gamma T_{i,N-2}-\beta T_{i+1,N}+\beta T_{i-1,N})}{(3k_T\gamma+2J\sqrt{\gamma}a_1x_{i,N}+2J\sqrt{\gamma}a_2y_{i,N}+2J\sqrt{\gamma}a_3)^2} \tag{14}$$

$$\frac{\partial T_{i,N}}{\partial a_2}=\frac{2J\sqrt{\gamma}y_{i,N}k_T(3T_{\infty_2}\gamma-4\gamma T_{i,N-1}+\gamma T_{i,N-2}-\beta T_{i+1,N}+\beta T_{i-1,N})}{(3k_T\gamma+2J\sqrt{\gamma}a_1x_{i,N}+2J\sqrt{\gamma}a_2y_{i,N}+2J\sqrt{\gamma}a_3)^2} \tag{15}$$

$$\frac{\partial T_{i,N}}{\partial a_3}=\frac{2J\sqrt{\gamma}k_T(3T_{\infty_2}\gamma-4\gamma T_{i,N-1}+\gamma T_{i,N-2}-\beta T_{i+1,N}+\beta T_{i-1,N})}{(3k_T\gamma+2J\sqrt{\gamma}a_1x_{i,N}+2J\sqrt{\gamma}a_2y_{i,N}+2J\sqrt{\gamma}a_3)^2} \tag{16}$$

Case 2) Temperature-dependent heat transfer coefficient $h_2(T_{\Gamma_2})=a+bT_{\Gamma_2}$:

In this case, the sensitivity of the objective function $\boldsymbol{\mathcal{J}}$ defined by Eq.(7) to the unknown variables a and b is calculated as follows

$$\frac{\partial \boldsymbol{\mathcal{J}}}{\partial a}=2C\sum_{i=2}^{M-1}(T_{i,N}-T_{(i,N)_m})\frac{\partial T_{i,N}}{\partial a}=2\sum_{i=2}^{M-1}(T_{i,N}-T_{(i,N)_m})C\frac{\partial T_{i,N}}{\partial a} \tag{17}$$

$$\frac{\partial \boldsymbol{\mathcal{J}}}{\partial b}=2C\sum_{i=2}^{M-1}(T_{i,N}-T_{(i,N)_m})\frac{\partial T_{i,N}}{\partial b}=2\sum_{i=2}^{M-1}(T_{i,N}-T_{(i,N)_m})C\frac{\partial T_{i,N}}{\partial b} \tag{18}$$

In a similar fashion, Eq. (12) becomes

$$-k_T\left[\frac{1}{J\sqrt{\gamma}}\left(\gamma\frac{3T_{i,N}-4T_{i,N-1}+T_{i,N-2}}{2}-\beta\frac{T_{i+1,N}-T_{i-1,N}}{2}\right)\right]=(a+bT_{i,N})\Big(T_{i,N}-T_{\infty_2}\Big) \tag{19}$$

Eq. (19) is a quadratic equation in terms of $T_{i,N}$. The following expression is obtained by solving Eq. (19) in terms of $T_{i,N}$:

$$T_{i,N} = -\frac{1}{4}\frac{1}{J\sqrt{\gamma}b}\Big(3k_T\gamma + 2J\sqrt{\gamma}a - 2J\sqrt{\gamma}bT_{\infty_2} - (9k_T^2\gamma^3 + 12k_T\gamma^{\frac{3}{2}}Ja - 12k_T\gamma^{\frac{3}{2}}JbT_{\infty_2} + 4J^2\gamma a^2$$

$$+8J^2\gamma abT_{\infty_2} + 4J^2\gamma b^2T_{\infty_2}^2 - 8J\sqrt{\gamma}bk_T\beta T_{i-1,N} + 32J\gamma^{\frac{3}{2}}bk_TT_{i,N-1} - 8J\gamma^{\frac{3}{2}}bk_TT_{i,N-2} + 8J\sqrt{\gamma}bk_T\beta T_{i+1,N})^{\frac{1}{2}}\Big) \quad (20)$$

Again, using an algebraic software, one can obtain an expression for the sensitivity coefficients $C\frac{\partial T_{i,N}}{\partial a}$ and $C\frac{\partial T_{i,N}}{\partial b}$ by differentiating the obtained expression for $T_{i,N}$ with respect to a and b, respectively, as follows

$$\frac{\partial T_{i,N}}{\partial a} =$$

$$-\frac{1}{4}\frac{1}{J\sqrt{\gamma}b}\Big(2J\sqrt{\gamma} - \frac{1}{2}(12k_T\gamma^{\frac{3}{2}}J + 8J^2\gamma a + 8J^2\gamma bT_{\infty_2}) / (9k_T^2\gamma^2 + 12k_T\gamma^{\frac{3}{2}}Ja - 12k_T\gamma^{\frac{3}{2}}JbT_{\infty_2} + 4J^2\gamma a^2 +$$

$$8J^2\gamma abT_{\infty_2} + 4J^2\gamma b^2T_{\infty_2}^2 - 8J\sqrt{\gamma}bk_T\beta T_{i-1,N} + 32J\gamma^{\frac{3}{2}}bk_TT_{i,N-1} - 8J\gamma^{\frac{3}{2}}bk_TT_{i,N-2} + 8J\sqrt{\gamma}bk_T\beta T_{i+1,N})^{\frac{1}{2}}\Big) \quad (21)$$

$$\frac{\partial T_{i,N}}{\partial b} =$$

$$-\frac{1}{4}\frac{1}{J\sqrt{\gamma}b}\Big(-2J\sqrt{\gamma}T_{\infty_2} - \frac{1}{2}(-12k_T\gamma^{\frac{3}{2}}JT_{\infty_2} + 8J^2\gamma aT_{\infty_2} + 8J^2\gamma bT_{\infty_2}^2 - 8J\sqrt{\gamma}k_T\beta T_{i-1,N}$$

$$+32J\gamma^{\frac{3}{2}}k_{T}T_{i,N-1}-8J\gamma^{\frac{3}{2}}k_{T}T_{i,N-2}+8J\sqrt{\gamma}bk_{T}\beta T_{i+1,N})\,/\,(9k_{T}^{2}\gamma^{2}+12k_{T}\gamma^{\frac{3}{2}}Ja-12k_{T}\gamma^{\frac{3}{2}}JbT_{\infty_{2}}+4J^{2}\gamma a^{2}+$$

$$8J^{2}\gamma abT_{\infty_{2}}+4J^{2}\gamma b^{2}T_{\infty_{2}}^{2}-8J\sqrt{\gamma}bk_{T}\beta T_{i-1,N}+32J\gamma^{\frac{3}{2}}bk_{T}T_{i,N-1}-8J\gamma^{\frac{3}{2}}bk_{T}T_{i,N-2}+8J\sqrt{\gamma}bk_{T}\beta T_{i+1,N})^{\frac{1}{2}}\Bigg) \tag{22}$$

Moreover, other forms of dependency of the heat transfer coefficient on the temperature, such as $h_{2}(T_{\Gamma_{2}})=a+bT_{\Gamma_{2}}+cT_{\Gamma_{2}}^{2}$ (quadratic) and $h_{2}(T_{\Gamma_{2}})=a+bT_{\Gamma_{2}}+cT_{\Gamma_{2}}^{2}+dT_{\Gamma_{2}}^{3}$ (cubic), may also be used resulting in a cubic and a quartic equation in terms of $T_{i,N}$, respectively. Hence one can obtain an expression for the sensitivity coefficients by differentiating the obtained expression for $T_{i,N}$ with respect to the coefficients appearing in the heat transfer coefficient expression (as there are algebraic expressions for the roots of cubic and quartic equations).

Using Eqs. (14)-(16), the sensitivity matrix **Ja** for Case 1 (space-dependent heat transfer coefficient) can be explicitly written as

$$\mathbf{Ja}_{a_1}=C\begin{bmatrix}\dfrac{\partial T_{2,N}}{\partial a_1}\\ \dfrac{\partial T_{3,N}}{\partial a_1}\\ \vdots\\ \dfrac{\partial T_{M-1,N}}{\partial a_1}\end{bmatrix}_{(M-2)\times 1},\mathbf{Ja}_{a_2}=C\begin{bmatrix}\dfrac{\partial T_{2,N}}{\partial a_2}\\ \dfrac{\partial T_{3,N}}{\partial a_2}\\ \vdots\\ \dfrac{\partial T_{M-1,N}}{\partial a_2}\end{bmatrix}_{(M-2)\times 1},\mathbf{Ja}_{a_3}=C\begin{bmatrix}\dfrac{\partial T_{2,N}}{\partial a_3}\\ \dfrac{\partial T_{3,N}}{\partial a_3}\\ \vdots\\ \dfrac{\partial T_{M-1,N}}{\partial a_3}\end{bmatrix}_{(M-2)\times 1} \tag{23}$$

And using Eqs. (21) and (22), the sensitivity matrix **Ja** for Case 2 (temperature-dependent heat transfer coefficient) can be explicitly written as

$$\mathbf{Ja}_a = C\begin{bmatrix} \dfrac{\partial T_{2,N}}{\partial a} \\ \dfrac{\partial T_{3,N}}{\partial a} \\ \vdots \\ \dfrac{\partial T_{M-1,N}}{\partial a} \end{bmatrix}_{(M-2)\times 1} , \mathbf{Ja}_b = C\begin{bmatrix} \dfrac{\partial T_{2,N}}{\partial b} \\ \dfrac{\partial T_{3,N}}{\partial b} \\ \vdots \\ \dfrac{\partial T_{M-1,N}}{\partial b} \end{bmatrix}_{(M-2)\times 1} \tag{24}$$

Problems for which the value of $\left|\mathbf{Ja}^{\mathrm{T}}\mathbf{Ja}\right|$ is very small are referred to as ill-conditioned. In general, IHTPs are very ill-conditioned particularly near the initial guess used for the unknown parameters which may be far from the actual solution. This may result in a negative value for the variable heat transfer coefficient and hence the termination of the iterative process. To circumvent this problem, the constant C is introduced in the objective function expression to be able to incorporate it into the sensitivity coefficients and form a new set of sensitivity coefficients.

3.3 The Conjugate Gradient Method (CGM)

In this study, the conjugate gradient optimization method is used due to its reliable performance in treating ~~the~~ inverse heat transfer problems. The objective function given by Eq. (7) is minimized by searching along the direction of descent $d^{(\mathrm{k})}$ using a search step size $\beta^{(\mathrm{k})}$.

$$f^{(\mathrm{k}+1)} = f^{(\mathrm{k})} - \beta^{(\mathrm{k})} d^{(\mathrm{k})} \tag{25}$$

where $f \equiv a_1, a_2, a_3$ for Case 1 and $f \equiv a, b$ for Case 2. The direction of descent of the current iteration is obtained as a linear combination of the direction of descent of the previous iteration and the gradient direction $\nabla \mathcal{J}^{(\mathrm{k})}$. Therefore,

$$d^{(\mathrm{k})} = \nabla \mathcal{J}^{(\mathrm{k})} + \gamma^{(\mathrm{k})} d^{(\mathrm{k}-1)} \tag{26}$$

The Polak-Ribiere formula [51] is employed to calculate the conjugation coefficient:

$$\gamma^{(\mathrm{k})} = \frac{\left[\nabla \boldsymbol{\mathcal{J}}^{(\mathrm{k})}\right]^{\mathrm{T}} (\nabla \boldsymbol{\mathcal{J}}^{(\mathrm{k})} - \nabla \boldsymbol{\mathcal{J}}^{(\mathrm{k}-1)})}{\| \nabla \boldsymbol{\mathcal{J}}^{(\mathrm{k}-1)} \|^2} = \frac{\left[\nabla \boldsymbol{\mathcal{J}}^{(\mathrm{k})}\right]^{\mathrm{T}} (\nabla \boldsymbol{\mathcal{J}}^{(\mathrm{k})} - \nabla \boldsymbol{\mathcal{J}}^{(\mathrm{k}-1)})}{\left[\nabla \boldsymbol{\mathcal{J}}^{(\mathrm{k}-1)}\right]^{\mathrm{T}} \nabla \boldsymbol{\mathcal{J}}^{(\mathrm{k}-1)}} \tag{27}$$

The search step size is given as follows [2]

$$\beta^{(\mathrm{k})} = \frac{[\mathbf{Ja}^{(\mathrm{k})} d^{(\mathrm{k})}]^{\mathrm{T}} [T_{i,N} - T_{(i,N)_m}]}{[\mathbf{Ja}^{(\mathrm{k})} d^{(\mathrm{k})}]^{\mathrm{T}} [\mathbf{Ja}^{(\mathrm{k})} d^{(\mathrm{k})}]} \tag{28}$$

The following algorithm represents the direct and inverse analysis steps used to estimate the space- and temperature-dependent heat transfer coefficient in steady-state heat conduction problems separately:

1. Specify the physical domain, the boundary conditions, and the measured outer surface temperature.

2. Generate the boundary-fitted grid using the elliptic grid generation method.

3. Solve the direct problem of finding the temperature values at any grid points of the physical domain using an initial variable heat transfer coefficient (initial guess for a_1, a_2, a_3 and a, b).

4. Using Eq. (7), compute the objective function ($\boldsymbol{\mathcal{J}}^{(\mathrm{k})}$).

5. If value of the objective function obtained in step 4 is less than the specified stopping criterion, the optimization is finished. Otherwise, go to step 6.

6. Compute the sensitivity matrices $\mathbf{Ja}_{a_1}$, $\mathbf{Ja}_{a_2}$, and $\mathbf{Ja}_{a_3}$ (for Case 1) from Eq. (23) and the sensitivity matrices $\mathbf{Ja}_a$ and $\mathbf{Ja}_b$ (for Case 2) from Eq. (24).

7. Compute the gradient directions $\nabla \boldsymbol{J}_{a_l}^{(\mathrm{k})}$ ($l = 1,2,3$) from Eq. (8) and $\nabla \boldsymbol{J}_{a}^{(\mathrm{k})}$ and $\nabla \boldsymbol{J}_{b}^{(\mathrm{k})}$ from Eqs. (17) and (18), respectively.

8. Compute the conjugation coefficients $\gamma_{a_l}^{(\mathrm{k})}$ ($l = 1,2,3$) and $\gamma_{a}^{(\mathrm{k})}$ and $\gamma_{b}^{(\mathrm{k})}$ from Eq. (27). For $\mathrm{k} = 0$, set $\gamma^{(0)} = 0$.

9. Compute the directions of descent $d_{a_l}^{(\mathrm{k})}$ ($l = 1,2,3$) and $d_{a}^{(\mathrm{k})}$ and $d_{b}^{(\mathrm{k})}$ from Eq. (26).

10. Compute the search step sizes $\beta_{a_l}^{(\mathrm{k})}$ ($l = 1,2,3$) and $\beta_{a}^{(\mathrm{k})}$ and $\beta_{b}^{(\mathrm{k})}$ from Eq. (28).

11. From Eq. (25), evaluate the new values for a_l ($l = 1,2,3$) and a and b separately, namely $a_1^{(\mathrm{k}+1)}$, $a_2^{(\mathrm{k}+1)}$, $a_3^{(\mathrm{k}+1)}$, and $a^{(\mathrm{k}+1)}$ and $b^{(\mathrm{k}+1)}$.

12. Set the next iteration ($\mathrm{k} = \mathrm{k} + 1$) and return to the step 2.

In Eq. (25), if the value of the expression $\beta^{(\mathrm{k})} d^{(\mathrm{k})}$ is larger than the value of $f^{(\mathrm{k})}$, then the new value for the variable heat transfer coefficient, $h_2^{(\mathrm{k}+1)} = a_1^{(\mathrm{k}+1)} x_{i,N} + a_2^{(\mathrm{k}+1)} y_{i,N} + a_3^{(\mathrm{k}+1)}$ $(i = 2, \cdots, M-1)$ or $h_2^{(\mathrm{k}+1)} = a^{(\mathrm{k}+1)} + b^{(\mathrm{k}+1)} T_{i,N}^{(\mathrm{k}+1)}$, becomes negative resulting in termination of the iterative process. Thus the parameter C is introduced in Eq. (6) to decrease the value of the expression $\beta^{(\mathrm{k})} d^{(\mathrm{k})}$ and obtain a positive value for the heat transfer coefficient in the next iteration, thereby continuing the iterative process. We start every problem with an ordinary least square objective function for which $n = 0, C = 1$. It is obvious that multiplication (or division) of the objective function value by a positive constant C will not change the optimum solution [52].

3.4 stopping criterion

If the problem involves no measurement errors, the traditional check condition is specified as

$$\mathcal{J}^{(\mathrm{k})} < \varepsilon \tag{29}$$

where ε is a small specified number. However, the measured temperatures will contain errors. In this case, the objective function value will not be zero at the end of the iterative process. As the computed temperatures approach the measured temperatures containing errors, during the minimization of the objective function (Eq. (7)), large oscillations may appear in the inverse problem solution resulting in an ill-posed character for the inverse problem. However, the conjugate gradient method may become well-posed if the *Discrepancy Principle* is used to stop the iterative procedure. In the Discrepancy Principle, the solution is assumed to be sufficiently accurate when the difference between computed and measured temperatures is of the order of magnitude of the measurement errors, that is,

$$\left| T_{\text{computed}} - T_{\text{measured}} \right| \approx \sigma \tag{30}$$

where σ is the standard deviation of the measurement errors, which is assumed constant in the present analysis. We can obtain the following value for ε by substituting Eq. (30) into Eq. (7) (objective function definition)

$$\varepsilon = C(M-2)\sigma^2 \tag{31}$$

Then the iterative procedure is stopped when the following criterion is satisfied [2]

$$\mathcal{J}^{(\mathrm{k})} < \varepsilon \tag{32}$$

4. Results

In this paper, two test cases are investigated to demonstrate the accuracy and efficiency of the proposed inverse analysis in the numerical treatment of inverse heat conduction problems involving variable heat transfer coefficient. Test Case 1 deals with a space-

dependent heat transfer coefficient and Test Case 2 treats a temperature-dependent heat transfer coefficient. It is first assumed that the variable heat transfer coefficient h_2 is known, the heat conduction problem is solved using the given boundary conditions to obtain the temperature distribution on the surface Γ_2. Then the computed temperature distribution $T_{i,N}$ ($i = 2,\ldots,M-1$) is used as the simulated measured temperatures for inverse analysis to recover the initially used variable heat transfer coefficient h_2. To avoid committing an *inverse crime*, a different mesh is also used to recover the desired parameter (h_2).

4.1 Space-dependent heat transfer coefficient:

As stated above, the steady-state heat conduction problem is initially solved using the known values for the thermal conductivity of conducting body k_T, the constant heat transfer coefficient h_i imposed on the surface Γ_i ($i = 3,4$), the space-dependent heat transfer coefficient $h_2 = 0.05x_{i,N} + 0.007y_{i,N} + 2.5$ imposed on the surface Γ_2, and the heat flux $\dot{q}$ applied on the surface Γ_1 to obtain the temperature distribution on the outer surface Γ_2 ($T_{i,N}$, $i = 2,\ldots,M-1$). To facilitate the computation of the sensitivity matrix coefficients using the central finite-difference relations, the grid nodes $(1,N)$ and (M,N) on corners of the outer surface Γ_2 are excluded from computing the temperature distribution. Then the resulting outer surface temperature distribution is used as the simulated measured temperatures in the inverse analysis to recover the initially used values for three parameters $a_1 = 0.05$, $a_2 = 0.007$, and $a_3 = 2.5$. To do so, the square of the difference between the temperature distribution of the outer surface Γ_2 (obtained from the solution the direct problem at each iteration) and the simulated measured temperature distribution of the same surface (Γ_2) is to be minimized.

Test Case 1: Numerical values of the coefficients involved in this test case are listed in Table 1. The temperature distribution in the body (using a grid size of 50×40) and the simulated measured temperature distribution on the outer surface Γ_2, $T_{(i,N)_m}$, are demonstrated in Fig. 3a and Fig. 3b, respectively. $T_{(i,N)_m}$ will be used in the inverse analysis to recover the initial values of a_1, a_2, a_3. Using an inverse analysis, the known (desired) values of $a_{1_d} = 0.05$, $a_{2_d} = 0.007$, and $a_{3_d} = 2.5$ are to be recovered by utilizing two different initial guesses:

$$a_{1_{\text{initial}_1}} = 0.00002, a_{2_{\text{initial}_1}} = 0.0004, a_{3_{\text{initial}_1}} = 0.00001$$

$$a_{1_{\text{initial}_2}} = 0.1, a_{2_{\text{initial}_2}} = 0.7, a_{3_{\text{initial}_2}} = -0.8$$

$\dot{q}(\frac{\text{W}}{\text{m}^2})$	$k_T(\frac{\text{W}}{\text{m.C}})$	$h_2(\frac{\text{W}}{\text{m}^2.\text{C}})$	$h_3(\frac{\text{W}}{\text{m}^2.\text{C}})$	$h_4(\frac{\text{W}}{\text{m}^2.\text{C}})$	$T_{\infty_2}(^\circ\text{C})$	$T_{\infty_3}(^\circ\text{C})$	$T_{\infty_4}(^\circ\text{C})$
2000	10	$0.05x_{i,N} + 0.007y_{i,N} + 2.5$	5	5	30	30	30

Table 1 Data used for Test Case 1.

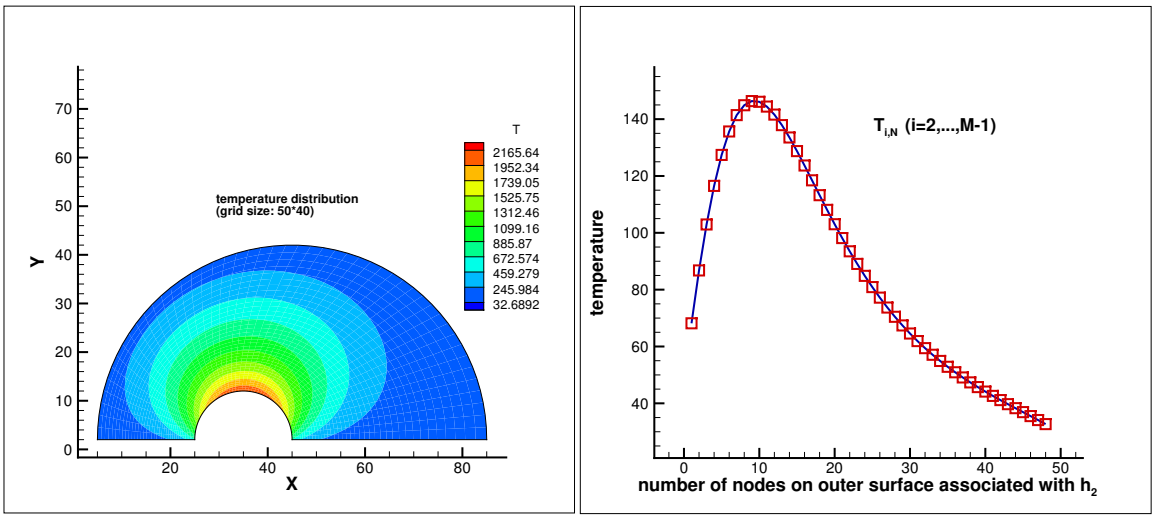

a) b)

Fig. 3 Temperature distribution in irregular physical domain (a) and on outer surface Γ_2 (used as T_m for inverse analysis) (b).

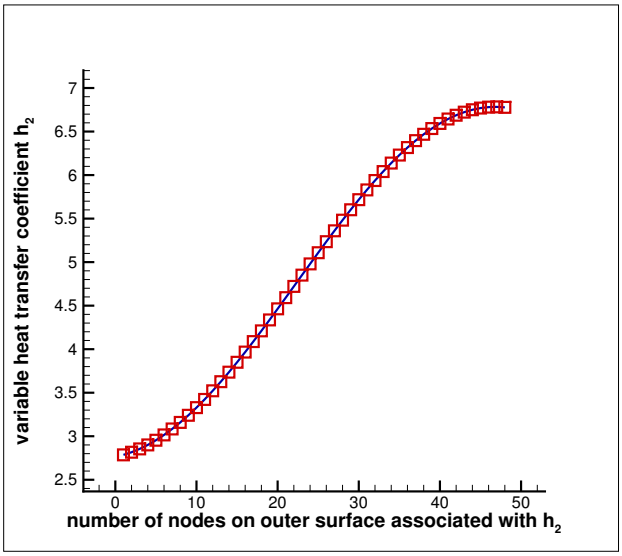

Fig. 4 Distribution of variable heat transfer coefficient on the outer surface Γ_2.

Initial guess 1: $h_{2_{\text{initial}_1}} = 0.00002x_{i,N} + 0.0004y_{i,N} + 0.00001(\frac{\text{W}}{\text{m}^2.\text{C}})$

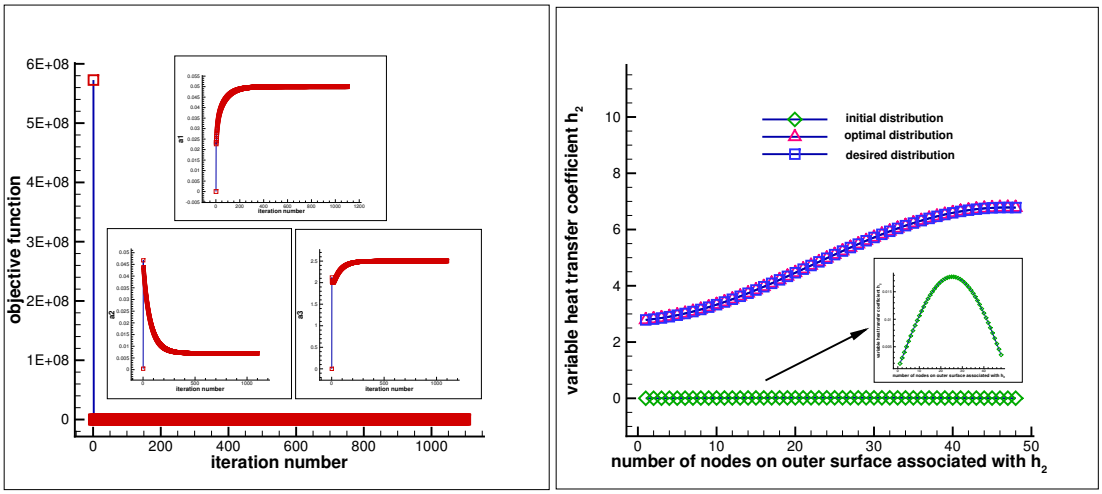

a) b)

Fig. 5 Estimation of a_1, a_2, a_3 ($h_2 = a_1 x_{i,N} + a_2 y_{i,N} + a_3$) and objective function versus iteration number for initial heat transfer coefficient $h_{2_{\text{initial}_1}} = 0.00002x_{i,N} + 0.0004y_{i,N} + 0.00001(\text{W}/\text{m}^2.\text{C})$ (a), and comparison of initial, optimal, and desired (simulated measured) heat transfer coefficient distributions (b).

Initial guess 2: $h_{2_{\text{initial}_2}} = 0.1x_{i,N} + 0.7y_{i,N} - 0.8(\frac{\text{W}}{\text{m}^2\,.\text{C}})$

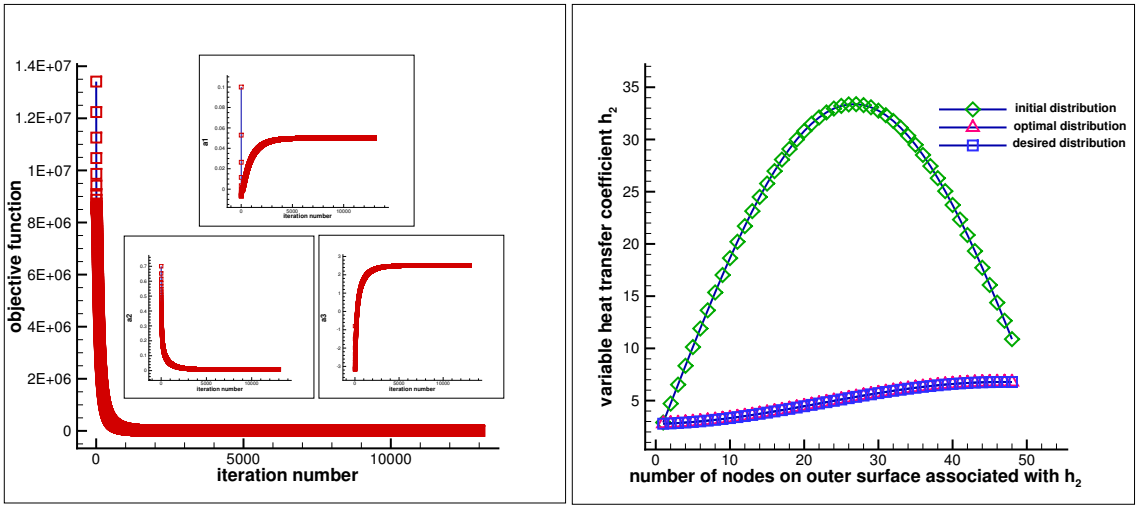

a) b)

Fig. 6 Estimation of a_1, a_2, a_3 ($h_2 = a_1 x_{i,N} + a_2 y_{i,N} + a_3$) and objective function versus iteration number for initial heat transfer coefficient $h_{2_{\text{initial}_2}} = 0.1x_{i,N} + 0.7y_{i,N} - 0.8(\text{W/ m}^2\,.\text{C})$ (a), and comparison of initial, optimal, and desired (simulated measured) heat transfer coefficient distributions (b).

The inverse analysis is investigated using two different initial guesses which are far from the desired ones. The initial guesses are selected so that they can reflect the accuracy, efficiency, and robustness of the inverse analysis. For the first initial guess, a different grid size (50×60) is used to avoid committing an *inverse crime*. The convergence history of the components of the variable heat transfer coefficient (a_1, a_2, a_3) and the decrease in the objective function versus the iteration number are shown in Fig. 5a (for initial 1), Fig. 6a (for initial 2), and Fig. 7a (for initial 2 with the measurement error). The comparison of the initial, optimal, and desired heat transfer coefficient distributions on the surface Γ_2 are shown in Fig. 5b (for initial 1), Fig. 6b (for initial 2), and Fig. 7b (for initial 2 with the measurement error). The details of the results, including the initial and final values for

a_1, a_2, a_3, the initial and final values of the objective function, the computation time, and the percentage of the decrease in the objective function are given in Table 2 (for both cases of no measurement error and a measurement error). As shown in Table 2, a 100% reduction in the objective function and complete recovering of the values for a_1, a_2, a_3 (the heat transfer coefficient components) are achieved in both initial cases with no measurement error. In case of the measurement error of $\sigma = 0.5$, there is also an approximately a 100% reduction in the objective function. As shown in Table 2, the errors in recovering the parameters a_1, a_2, a_3 are insignificant. The results are obtained by a FORTRAN compiler and computations are run on a PC with Intel Core i5 and 6G RAM. A tolerance of 10^{-7} is used in iterative loops to increase the accuracy of results.

Initial guess 2 (with measurement error): $h_{2_{\text{initial}_2}} = 0.1x_{i,N} + 0.7y_{i,N} - 0.8(\frac{\text{W}}{\text{m}^2.\text{C}})$

In this study, for both cases of space- and temperature-dependent heat transfer coefficient, the measured temperature containing random errors, $T_{i,N}^{\text{meas}}$ $(i = 2,\ldots,M-1)$, is generated by adding an error term $\omega\sigma$ to the exact temperature $T_{i,N}^{\text{exact}}$ to give

$$T_{i,N}^{\text{meas}} = T_{i,N}^{\text{exact}} + \omega\sigma \tag{33}$$

where ω is a random variable with normal distribution, zero mean, and unitary standard deviation. Assuming 99% confidence for the measured temperature, ω lies in the range $-2.576 \leq \omega \leq 2.576$ and it is randomly generated by using MATLAB. σ is the standard deviation of the measurement errors and is considered as $\sigma = 0.5$ in this study. The initial guess 2 ($h_{2_{\text{initial}_2}} = 0.1x_{i,N} + 0.7y_{i,N} - 0.8(\frac{\text{W}}{\text{m}^2.\text{C}})$) is considered again to initiate the optimization process.

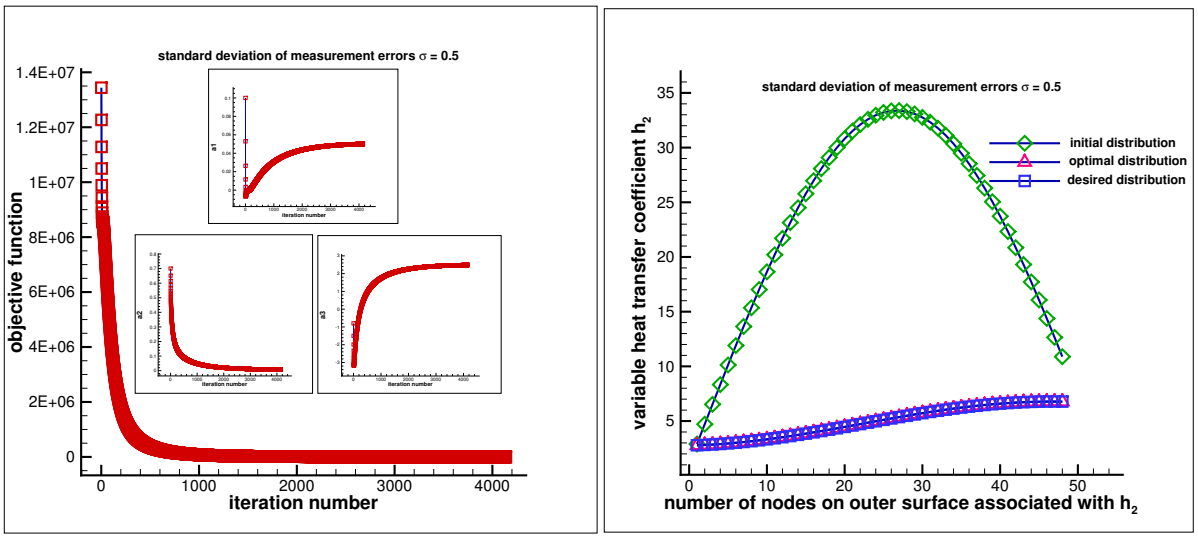

a) b)

Fig. 7 Estimation of a_1, a_2, a_3 ($h_2 = a_1 x_{i,N} + a_2 y_{i,N} + a_3$) and objective function versus iteration number for initial heat transfer coefficient $h_{2_{\text{initial}_2}} = 0.1x_{i,N} + 0.7y_{i,N} - 0.8(\text{W/ m}^2\text{.C})$ by considering measurement error (a), and comparison of initial, optimal, and desired (simulated measured) heat transfer coefficient distributions (b).

Grid size	Desired value	Initial (guess) value	Final value	Temperature measurement error	Initial value of $\mathcal{J}$	Minimum value of $\mathcal{J}$	Reduction in objective function & computation time
50×60	$a_1 = 0.05$ $a_2 = 0.007$ $a_3 = 2.5$	$a_1 = 0.00002$ $a_2 = 0.0004$ $a_3 = 0.00001$	$a_1 = 5.00\times10^{-2}$ $a_2 = 6.96\times10^{-3}$ $a_3 = 2.50$	$\sigma = 0$	572667842.97 $(C = 10)$	7.04×10^{-3}	100% (34s) (1100 iterations)
50×40		$a_1 = 0.1$ $a_2 = 0.7$ $a_3 = -0.8$	$a_1 = 5.00\times10^{-2}$ $a_2 = 7.00\times10^{-3}$ $a_3 = 2.50$	$\sigma = 0$	13410671.43 $(C = 100)$	8.21×10^{-6}	100% (4m:52s) (13000 iterations)
50×40		$a_1 = 0.1$ $a_2 = 0.7$ $a_3 = -0.8$	$a_1 = 5.01\times10^{-2}$ (error=0.2%) $a_2 = 7.34\times10^{-3}$ (error=4.86%) $a_3 = 2.49$ (error=0.4%)	$\sigma = 0.5$	13439285.83 $(C = 100)$	1199.87	~ 100% (4138 iterations)

Table 2 Results for the estimation the heat transfer coefficient components a_1, a_2, and a_3.

4.2 Temperature-dependent heat transfer coefficient:

Test Case 2: Numerical values of the coefficients involved in this test case are listed in Table 3. Initially the direct problem is solved using the known values for the thermal conductivity, the heat flux, and the heat transfer coefficients to obtain the temperature distribution on the outer surface Γ_2 (Fig. 8a), $T_{i,N}$, which will be used as the simulated measured temperatures $T_{(i,N)_m}$ for the inverse analysis to recover the initial values of a and b. The grid size is 60×50. Using an inverse analysis, the known (desired) values of $a_d = 6.0$ and $b_d = 0.4$ are to be recovered by utilizing two different initial guesses:

$$a_{\text{initial}_1} = 0.001, b_{\text{initial}_1} = 0.04$$

$$a_{\text{initial}_2} = 10.0, b_{\text{initial}_2} = 0.9$$

$\dot{q}(\frac{\text{W}}{\text{m}^2})$	$k_T(\frac{\text{W}}{\text{m.C}})$	$h_2(\frac{\text{W}}{\text{m}^2.\text{C}})$	$h_3(\frac{\text{W}}{\text{m}^2.\text{C}})$	$h_4(\frac{\text{W}}{\text{m}^2.\text{C}})$	$T_{\infty_2}(^\circ\text{C})$	$T_{\infty_3}(^\circ\text{C})$	$T_{\infty_4}(^\circ\text{C})$
1000	30	$6.0 + 0.4T_{i,N}$	7	7	20	20	20

Table 3 Data used for Test Case 2.

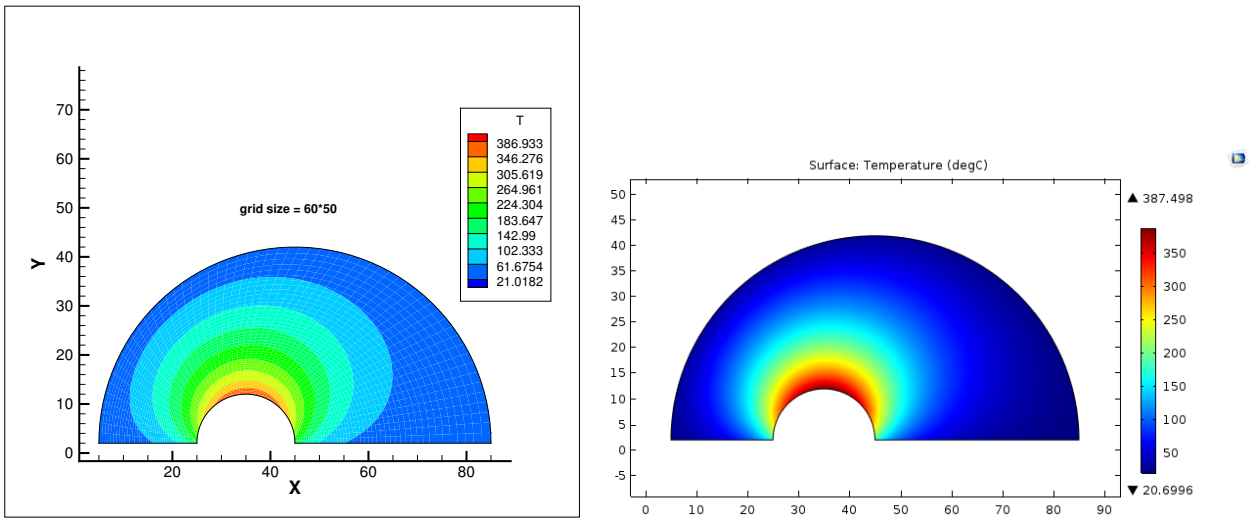

a) b)

Fig. 8 The validation of the implemented numerical method for the direct heat transfer problem using the finite element analysis software COMSOL. Temperature distribution obtained by the proposed numerical method (a) and temperature distribution obtained by COMSOL (b).

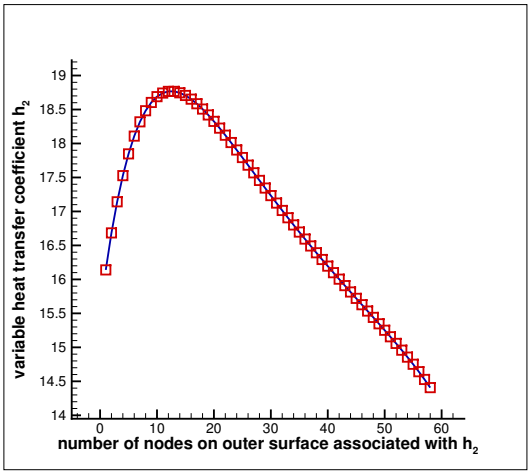

Fig. 9 Distribution of variable heat transfer coefficient on the outer surface Γ_2.

Initial guess 1: $h_{2_{\text{initial}_1}} = 0.001 + 0.04T_{i,N}(\frac{\text{W}}{\text{m}^2.\text{C}})$

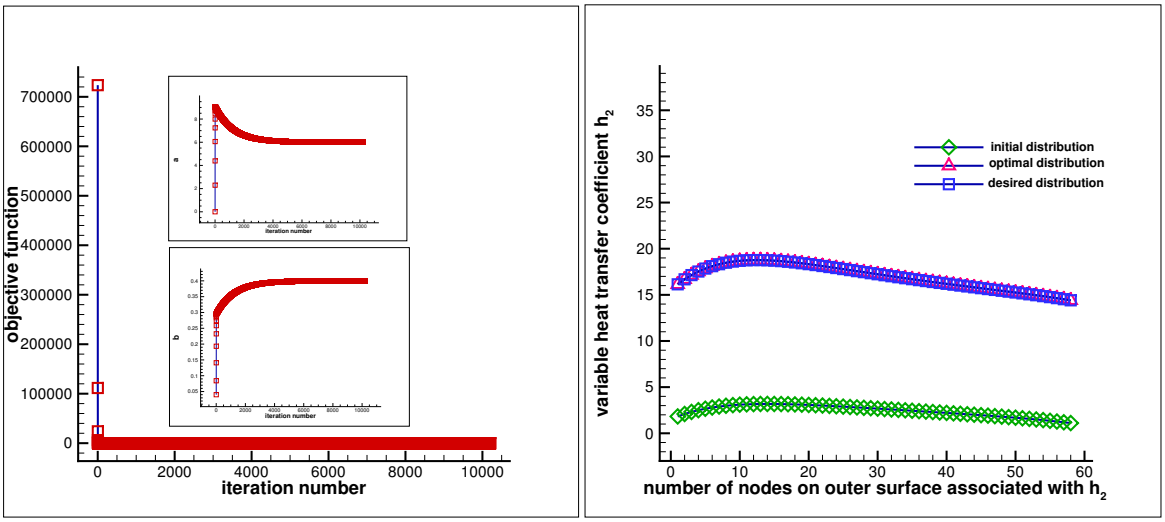

a) b)

Fig. 10 Estimation of a and b ($h_2 = a + bT_{i,N}$) and objective function versus iteration number for initial heat transfer coefficient $h_{2_{\text{initial}_1}} = 0.001 + 0.04T_{i,N}(\text{W/ m}^2.\text{C})$ (a), and comparison of initial, optimal, and desired (simulated measured) heat transfer coefficient distributions (b).

Initial guess 2: $h_{2_{\text{initial}_2}} = 10.0 + 0.9T_{i,N}(\dfrac{\text{W}}{\text{m}^2\,.\text{C}})$

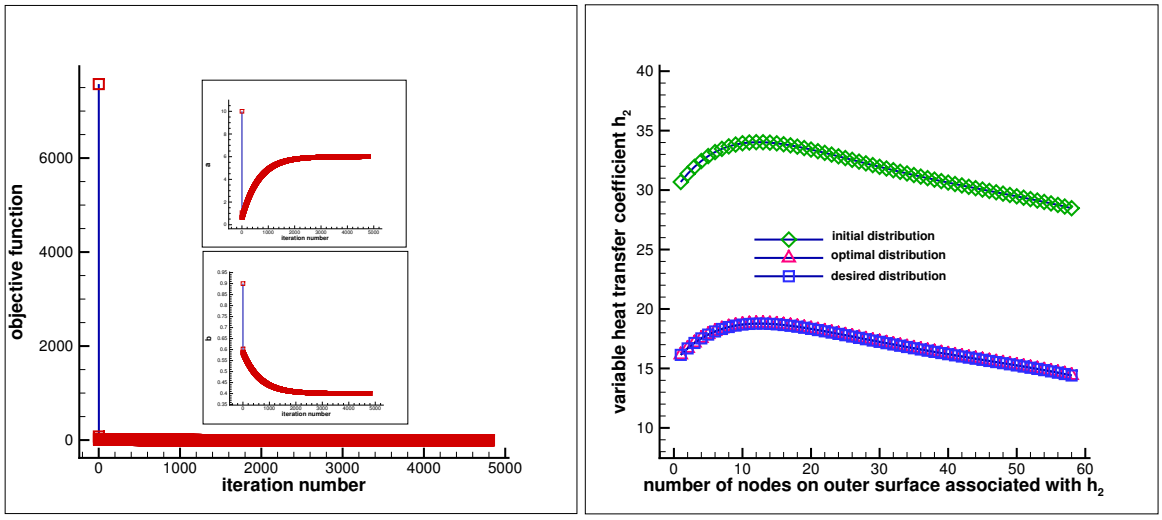

a) b)

Fig. 11 Estimation of a and b ($h_2 = a + bT_{i,N}$) and objective function versus iteration number for initial heat transfer coefficient $h_{2_{\text{initial}_2}} = 10.0 + 0.9T_{i,N}(\text{W}/\,\text{m}^2\,.\text{C})$ (a), and comparison of initial, optimal, and desired (simulated measured) heat transfer coefficient distributions (b).

Initial guess 2 (with measurement error): $h_{2_{\text{initial}_2}} = 10.0 + 0.9T_{i,N}(\frac{\text{W}}{\text{m}^2.\text{C}})$

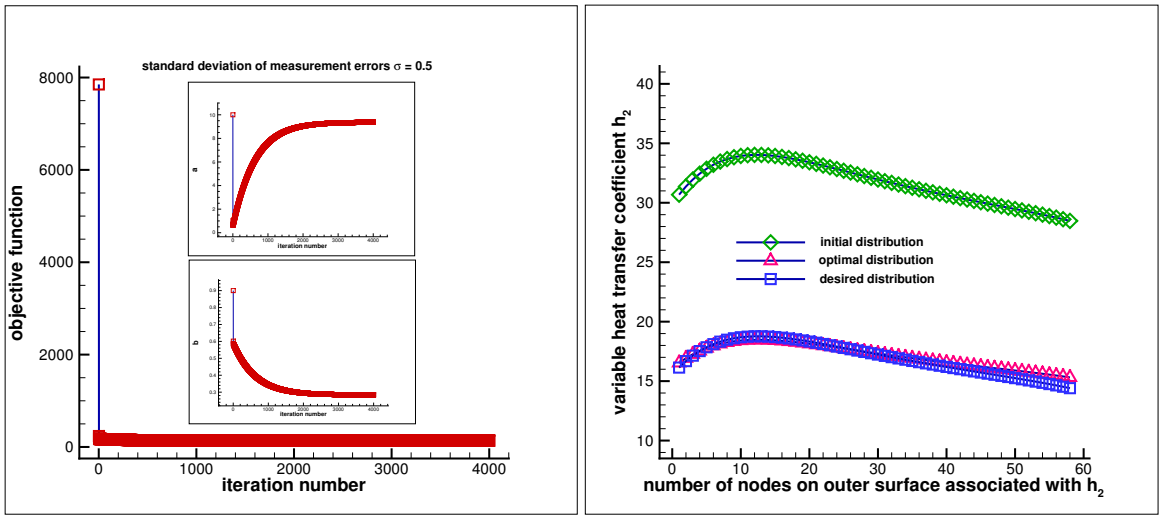

a) b)

Fig. 12 Estimation of a and b ($h_2 = a + bT_{i,N}$) and objective function versus iteration number for initial heat transfer coefficient $h_{2_{\text{initial}_2}} = 10.0 + 0.9T_{i,N}(\text{W}/\text{m}^2.\text{C})$ by considering measurement error (a), and comparison of initial, optimal, and desired (simulated measured) heat transfer coefficient distributions (b).

Grid size	Desired value	Initial (guess) value	Final value	Temperature measurement error	Initial value of $\mathcal{J}$	Minimum value of $\mathcal{J}$	Reduction in objective function & computation time
60×30	$a=6.0$ $b=0.4$	$a=0.001$ $b=0.04$	$a=6.0$ $b=0.4$	$\sigma=0$	723557.90 $(C=10)$	4.28×10^{-3}	100% (3 m : 41s) (10200 iterations)
60×80		$a=10.0$ $b=0.9$	$a=6.0$ $b=0.4$	$\sigma=0$	7574.36 $(C=10)$	4.32×10^{-4}	100% (5m:13s) (4800 iterations)
60×80		$a=10.0$ $b=0.9$	$a=9.36$ (error=56%) $b=0.28$ (error=29.25%)	$\sigma=0.5$	7850.54 $(C=10)$	136.35	~ 100% (4000 iterations)

Table 4 Results for the estimation the heat transfer coefficient components a and b.

Like the estimation of the space-dependent heat transfer coefficient, the inverse analysis used for estimation of the temperature-dependent heat transfer coefficient is investigated using two different initial guesses which are far from the desired ones. For both initial guesses, different grid sizes (60×30 for the initial 1 and 60×80 for initial 2 and initial 2 with measurement error) used to avoid committing an *inverse crime.* The convergence history of the components of the variable heat transfer coefficient (a,b) and the decrease in the objective function versus the iteration number are shown in Fig. 10a (for initial 1), Fig. 11a (for initial 2), and Fig. 12a (for initial 2 with the measurement error). The comparison of initial, optimal, and desired heat transfer distributions on the surface Γ_2 are shown in Fig. 10b (for initial 1), Fig. 11b (for initial 2), and Fig. 12b (for initial 2 with the measurement error). The details of the results, including the initial and final values for a,b, the initial and final values of the objective function, the computation time, and the percentage of the decrease in the objective function are given in Table 4 (for both cases of no measurement error and a measurement error). As shown in Table 4, a 100% reduction in the objective function and complete recovering of the values for a,b (the heat transfer coefficient components) are achieved in both initial cases with no measurement error. In case of the measurement error of $\sigma=0.5$, there is also an approximately a 100% reduction in the objective function. As shown in Table 4, the errors in recovering the parameters a,b are significant.

5. Conclusion

This paper presented a new numerical procedure for *separate* estimation of a space- and temperature-dependent heat transfer coefficient in a two dimensional irregular heat-conducting body using an inverse steady-state heat conduction analysis. The irregular body was transformed into a regular computational domain to perform all computations related to the direct and inverse heat conduction solution. To do this, an elliptic grid generation

scheme was used to generate a grid over the body. An accurate and very efficient sensitivity analysis scheme was used to calculate sensitivity coefficients needed in a gradient-based optimization method (here, conjugate gradient method). The explicit expressions for the sensitivity coefficients were derived for both dependence cases (space- and temperature- dependence) which allow for the computation of the sensitivity coefficients in one single solve, regardless of the number of unknown quantities. The conjugate gradient method was used as a tool to minimize the objective function and recover the desired quantities. The obtained results revealed that the proposed algorithm is very accurate and efficient.

6. References

[1] Alifanov O.M., Inverse Heat Transfer Problems, Springer-Verlag, 1994.

[2] Özisiķ M., Orlande H., Inverse Heat Transfer: Fundamentals and Applications, Taylor & Francis 2000.

[3] Beck J.V., Blackwell B., Clair C.R.S., Inverse Heat Conduction: Ill-Posed Problems, Wiley, 1985.

[4] Artyukhin E., Reconstruction of the thermal conductivity coefficient from the solution of the nonlinear inverse problem, Journal of Engineering Physics and Thermophysics, 41 (1981) 1054-1058.

[5] Alifanov O.M., Tryanin A.P., Determination of the coefficient of internal heat exchange and the effective thermal conductivity of a porous solid on the basis of a nonstationary experiment, Journal of Engineering Physics, 48 (1985) 356-365.

[6] Dantas L., Orlande H., A function estimation approach for determining temperature-dependent thermophysical properties, Inverse Problems in Engineering, 3 (1996) 261-279.

[7] Jurkowski T., Jarny Y., Delaunay D., Estimation of thermal conductivity of thermoplastics under moulding conditions: an apparatus and an inverse algorithm, International journal of heat and mass transfer, 40 (1997) 4169-4181.

[8] Yang C.-Y., A linear inverse model for the temperature-dependent thermal conductivity determination in one-dimensional problems, Applied Mathematical Modelling, 22 (1998) 1-9.
[9] Divo E., Kassab A.J., Kapat J.S., Chyu M.-K., Retrieval of multidimensional heat transfer coefficient distributions using an inverse BEM-based regularized algorithm: numerical and experimental results, Engineering Analysis with Boundary Elements, 29 (2005) 150-160.
[10] Sawaf B., Ozisik M.N., Jarny Y., An inverse analysis to estimate linearly temperature dependent thermal conductivity components and heat capacity of an orthotropic medium, International Journal of Heat and Mass Transfer, 38 (1995) 3005-3010.
[11] Liu F.-B., A hybrid method for the inverse heat transfer of estimating fluid thermal conductivity and heat capacity, International Journal of Thermal Sciences, 50 (2011) 718-724.
[12] Zhang J., Delichatsios M.A., Determination of the convective heat transfer coefficient in three-dimensional inverse heat conduction problems, Fire Safety Journal, 44 (2009) 681-690.
[13] Chen W.-L., Yang Y.-C., Lee H.-L., Inverse problem in determining convection heat transfer coefficient of an annular fin, Energy Conversion and Management, 48 (2007) 1081-1088.
[14] Mierzwiczak M., Kołodziej J.A., The determination temperature-dependent thermal conductivity as inverse steady heat conduction problem, International Journal of Heat and Mass Transfer, 54 (2011) 790-796.
[15] Czél B., Gróf G., Inverse identification of temperature-dependent thermal conductivity via genetic algorithm with cost function-based rearrangement of genes, International Journal of Heat and Mass Transfer, 55 (2012) 4254-4263.
[16] Huang C.-H., Jan-Yuan Y., An inverse problem in simultaneously measuring temperature-dependent thermal conductivity and heat capacity, International Journal of Heat and Mass Transfer, 38 (1995) 3433-3441.
[17] Yang C.-y., Estimation of the temperature-dependent thermal conductivity in inverse heat conduction problems, Applied Mathematical Modelling, 23 (1999) 469-478.

[18] Mohebbi F., Sellier M., Parameter estimation in heat conduction using a two-dimensional inverse analysis, International Journal for Computational Methods in Engineering Science and Mechanics, 17 (2016) 274-287.
[19] Tervola P., A method to determine the thermal conductivity from measured temperature profiles, International Journal of Heat and Mass Transfer, 32 (1989) 1425-1430.
[20] Huang C.H., Özişik M.N., Direct integration approach for simultaneously estimating temperature dependent thermal conductivity and heat capacity, Numerical Heat Transfer, Part A: Applications, 20 (1991) 95-110.
[21] Kim S., A simple direct estimation of temperature-dependent thermal conductivity with kirchhoff transformation, International Communications in Heat and Mass Transfer, 28 (2001) 537-544.
[22] Lin J.-H., Cha, Chen O.K., Yang Y.-T., Inverse Method for Estimating Thermal Conductivity in One-Dimensional Heat Conduction Problems, Journal of thermophysics and heat transfer, 15 (2001) 34-41.
[23] Chantasiriwan S., Steady-state determination of temperature-dependent thermal conductivity, International Communications in Heat and Mass Transfer, 29 (2002) 811-819.
[24] Liu C.-S., One-step GPS for the estimation of temperature-dependent thermal conductivity, International Journal of Heat and Mass Transfer, 49 (2006) 3084-3093.
[25] Sawaf B., Özisik M.N., Determining the constant thermal conductivities of orthotropic materials by inverse analysis, International Communications in Heat and Mass Transfer, 22 (1995) 201-211.
[26] Lam T.T., Yeung W.K., Inverse determination of thermal conductivity for one-dimensional problems, Journal of thermophysics and heat transfer, 9 (1995) 335-344.
[27] Lesnic D., Elliott L., Ingham D.B., Identification of the Thermal Conductivity and Heat Capacity in Unsteady Nonlinear Heat Conduction Problems Using the Boundary Element Method, Journal of Computational Physics, 126 (1996) 410-420.
[28] Mohebbi F., Sellier M., Rabczuk T., Estimation of linearly temperature-dependent thermal conductivity using an inverse analysis, International Journal of Thermal Sciences, 117 (2017) 68-76.

[29] Mohebbi F., Sellier M., Estimation of thermal conductivity, heat transfer coefficient, and heat flux using a three dimensional inverse analysis, International Journal of Thermal Sciences, 99 (2016) 258-270.
[30] Beck J.V., Surface heat flux determination using an integral method, Nuclear Engineering and Design, 7 (1968) 170-178.
[31] Huang C.H., Wang S.P., A three-dimensional inverse heat conduction problem in estimating surface heat flux by conjugate gradient method, International Journal of Heat and Mass Transfer, 42 (1999) 3387-3403.
[32] Liu F.-B., Inverse estimation of wall heat flux by using particle swarm optimization algorithm with Gaussian mutation, International Journal of Thermal Sciences, 54 (2012) 62-69.
[33] Yang Y.-C., Chen W.-L., A nonlinear inverse problem in estimating the heat flux of the disc in a disc brake system, Applied Thermal Engineering, 31 (2011) 2439-2448.
[34] Yang Y.-T., Hsu P.-T., Chen C.o.-K., A three-dimensional inverse heat conduction problem approach for estimating the heat flux and surface temperature of a hollow cylinder, Journal of Physics D: Applied Physics, 30 (1997) 1326.
[35] Huang C.-H., Chen W.-C., A three-dimensional inverse forced convection problem in estimating surface heat flux by conjugate gradient method, International Journal of Heat and Mass Transfer, 43 (2000) 3171-3181.
[36] Golbahar Haghighi M.R., Malekzadeh P., Rahideh H., Vaghefi M., Inverse Transient Heat Conduction Problems of a Multilayered Functionally Graded Cylinder, Numerical Heat Transfer, Part A: Applications, 61 (2012) 717-733.
[37] Hsieh C.K., Kassab A.J., A general method for the solution of inverse heat conduction problems with partially unknown system geometries, International Journal of Heat and Mass Transfer, 29 (1986) 47-58.
[38] Dulikravich G., Martin T., Inverse shape and boundary condition problems and optimization in heat conduction, Advances in Numerical Heat Transfer, 1 (1996) 381-426.
[39] Mohebbi F., Sellier M., Optimal shape design in heat transfer based on body-fitted grid generation, International Journal for Computational Methods in Engineering Science and Mechanics, 14 (2013) 227-243.

[40] Mohebbi F., Sellier M., Three-dimensional optimal shape design in heat transfer based on body-fitted grid generation, International Journal for Computational Methods in Engineering Science and Mechanics, 14 (2013) 473-490.
[41] Sarvari S.M.H., Optimal geometry design of radiative enclosures using the genetic algorithm, Numerical Heat Transfer, Part A: Applications, 52 (2007) 127-143.
[42] Wu C.-H.C.C.-Y., An approach combining body-fitted grid generation and conjugate gradient methods for shape design in heat conduction problems, Numerical Heat Transfer, Part B: Fundamentals, 37 (2000) 69-83.
[43] Mohebbi F., Sellier M., Rabczuk T., Inverse problem of simultaneously estimating the thermal conductivity and boundary shape, International Journal for Computational Methods in Engineering Science and Mechanics, (2017) 1-16.
[44] Kreith F., Manglik R.M., Bohn M.S., Principles of Heat Transfer, Cengage Learning, 2010.
[45] Louahlia-Gualous H., Panday P., Artioukhine E., Inverse determination of the local heat transfer coefficients for nucleate boiling on a horizontal cylinder, Journal of Heat Transfer, 125 (2003) 1087-1095.
[46] Beck J., Osman A., Nonlinear inverse problem for the estimation of time-and-space-dependent heat-transfer coefficients, Journal of thermophysics and heat transfer, 3 (1989) 146-152.
[47] Taler J., Determination of local heat transfer coefficient from the solution of the inverse heat conduction problem, Forschung im Ingenieurwesen, 71 (2007) 69-78.
[48] Martin T., Dulikravich G., Inverse determination of steady heat convection coefficient distributions, TRANSACTIONS-AMERICAN SOCIETY OF MECHANICAL ENGINEERS JOURNAL OF HEAT TRANSFER, 120 (1998) 328-334.
[49] Özişik M., Finite difference methods in heat transfer, CRC Press, 1994.
[50] Mohebbi F., Optimal shape design based on body-fitted grid generation (PhD thesis-link: http://hdl.handle.net/10092/9427), in, University of Canterbury 2014.
[51] Polak E., Ribiere G., Note sur la convergence de méthodes de directions conjuguées, Revue Française d'Informatique et de Recherche Opérationnelle, 16 (1969) 35–43.
[52] Rao S.S., Engineering Optimization: Theory and Practice, Wiley, 2009.